Journal of the European Ceramic Society 22 (2002) 2479–2487
www.elsevier.com/locate/jeurceramsoc

Non-cavitation tensile creep in Lu-doped silicon nitride

Frantisek Lofaj[a,*], Sheldon M. Wiederhorn[b], Gabrielle G. Long[b], Bernard J. Hockey[b], Pete R. Jemian[c], Lisa Browder[d], Jonathan Andreason[e], Ulrike Täffner[f]

[a]*Institute of Materials Research of the Slovak Academy of Sciences, 043 53 Kosice, Slovakia*
[b]*National Institute of Standards and Technology, Gaithersburg, MD 20899, USA*
[c]*University of Illinois at Urbana-Champaign/Argonne National Laboratory, IL 60439, USA*
[d]*Knox College, Galesburg, IL 61401, USA*
[e]*Illinois State University, Lincoln, IL 62656, USA*
[f]*Max-Planck-Institut für Metalkunde, Seestrasse 92, D-70174 Stuttgart, Germany*

Received 19 December 2001; received in revised form 1 April 2002; accepted 14 April 2002

Abstract

The tensile creep behavior of a Lu-doped silicon nitride was studied in the temperature range 1400–1550 °C with test periods of up to 10 200 h. Strain rates were 3–4 orders of magnitude less than those for Yb-doped grades of silicon nitride under the same conditions, suggesting a potential for prolonged operation of this material at temperatures up to 1470 °C. The stress exponent, n, and the activation energy, Q, for creep are 5.3 ± 2.0 and (757 ± 117) kJ/mol, respectively. Precise density and ultra-small-angle X-ray scattering measurements revealed that, in contrast to other grades of silicon nitride, cavitation could not be detected in the material studied. Redistribution of the secondary phases via solution-precipitation combined with grain boundary sliding is discussed as a possible creep mechanism. A discussion of the effect of Lu on viscosity indicates that replacement of Y by Lu may explain the improvement of creep behavior. © 2002 Published by Elsevier Science Ltd.

Keywords: Silicon nitride; Tensile creep; Lutetium; Cavity suppression; Solution-precipitation

1. Introduction

The maximum allowable turbine inlet temperature limits the efficiency of gas turbines. During the past three decades, turbine inlet temperatures in conventional gas turbines increased on average by 500 °C.[1] In the near future, the introduction of special types of blade cooling combined with thermal barrier coatings are expected to increase the turbine inlet temperature by another 230–330 °C, to as high as 1650 °C.[1–3] While these techniques may work for larger (>1 MW) power generating turbines, internal cooling of the blades is technologically unfeasible for small components in low-power turbines. Thus, the requirement for structural materials that can sustain high temperatures without cooling is a critical issue in the development of small high-efficiency gas turbines.

Structural ceramics, particularly silicon nitride, are candidate materials for components in low-power gas turbines because of their good mechanical properties at high temperatures. Tests of a Japanese 300 kW ceramic gas turbine, CGT 302, demonstrated the feasibility of an operating temperature of 1400 °C with a thermal efficiency of 42%.[4,5] This is twice the efficiency of a comparable metallic turbine. However, this turbine operated at 1400 °C for only 200 h[4,5] which is insufficient time to prove their reliability for industrial application. Research efforts in the USA have been concentrated on retrofitting conventional stationary gas turbines with ceramic parts.[6,7] Preliminary results confirmed some of the benefits expected from ceramic components, however, problems with the effects of environment and foreign object damage limit their commercial applicability in gas turbines.[7]

* Corresponding author. Tel.: +421-55-633-8115; fax: +421-55-633-7108.
E-mail address: lofaj@saske.sk (F. Lofaj).

0955-2219/02/$ - see front matter © 2002 Published by Elsevier Science Ltd.
PII: S0955-2219(02)00106-1

Creep resistance of the current generation of Y- and Yb-doped silicon nitride ceramics [for example, hot isostatically pressed (HIP-ed) NT 154[1],[8–10] or gas-pressure-sintered SN 88[2],[11–17]][3] is sufficient for long-term operation (>10 000 h) at temperatures as high as 1325 °C. To achieve higher temperatures, however, the development of more creep resistant grades of material for small engines is desirable.

Preliminary studies on newer Lu_2O_3 containing silicon nitrides, SN 281[4],[12,18–21] and SN 282,[22] indicate a decrease in creep rate and an increase in lifetime of up to two orders of magnitude. Lu_2O_3 in SN 281 and SN 282 may be responsible for the improvement in creep behavior. However, neither the reason for such a dramatic increase in creep resistance nor the mechanisms controlling creep behavior are well understood. The aim of the current work is to present some new data to clarify possible creep mechanisms in silicon nitrides with Lu-doped sintering aids.

2. Experimental procedure

2.1. Tensile creep testing

The material studied was a HIP-ed grade of silicon nitride, SN 281. Tensile creep tests were performed on flat, dog-bone shaped specimens designated as SR 51 type by French and Wiederhorn.[23] The gauge size of the specimens was 2 mm×2.5 mm and the gage length was 15 mm. They were loaded via single pin SiC pull rods using a commercial creep machine with dead weight loading (Model TCS 300X, Satec Systems, Inc., Groove City, PA). Tensile strain during creep was measured in situ using a laser-extensometer system to detect pair of silicon carbide flags hanging by their own weight from the specimen. The raw data were recorded on a computer in time intervals of 1, 5 or 15 min and were averaged over a time period corresponding to 3–7 data points. Details of the testing procedure are given elsewhere.[14,23]

2.2. Microstructure characterization

The phase composition of the material (as received and after testing) was investigated by X-ray diffraction (Cu K_α, $\lambda = 1.54046$ Å) from different areas of the bulk samples. The interior of the specimens, revealed by grinding away half of the specimen thickness, was used as a representative composition for the evaluation of changes in the bulk. The volume fraction of the second phase was measured on polished and plasma-etched specimens using the point count method.[24] The mean and standard deviation of the mean were determined from 20 randomly selected areas from the polished surface. Twenty different micrographs were used for the analysis. The line-intercept method was used to determine the grain size;[24] the mean intercept of a series of random lines on 13 randomly selected areas from the polished surface is reported as the grain size.

The samples for transmission electron microscopy (TEM) studies were prepared from five creep-tested specimens. They were cut from the core of the gauge section parallel to the direction of the applied stress. After hand grinding and polishing to approximately 100 μm thickness and dimpling, the foils were thinned by ion milling at 5 kV using Ar gas until foil perforation. Transmission electron microscopy investigations on carbon-coated specimens were carried out at 200 kV (Model 3010, Jeol Inc., Japan).

Creep damage was investigated by scanning electron microscopy (SEM) on secondary fracture surfaces produced at room temperature after creep and on polished and plasma etched cross sections.

2.3. Density measurement

The sink–float technique was used for the measurement of specimen density. Bars were cut from the gauge and grip section of five specimens after creep testing. They were then ground to remove the oxide layer at the surface. The final size of the samples was approximately 2.3 mm×1.7 mm×10 mm. Samples were put into a water solution of thallium malonate formate contained in a water-jacketed test-tube connected to the constant temperature bath. Two float standards (3.340 and 3.400 certified to ±0.0005 g/cm^3 by Cargille Corp., Cedar Grove, NJ) were added to the solution. The standards bracketed the expected density of the specimens. The density of the solution was initially adjusted by adding or by evaporating a small amount of water in such a way that the heavy standard just sank at room temperature. By adjusting the temperature of the water in the jacket, it was possible to bracket the buoyancy temperature of each specimen and standard to an accuracy of 0.5 °C. The density of the specimens was then calculated from the measured buoyancy temperature.[10] During the tests, a 3–5 mm thick layer of heptane prevented evaporation of the water from the test chamber. The layer was removed after each test by suctioning and evaporation.

The density change from creep strain was assumed to be equivalent to the volume fraction of cavities, f_v,

[1] St. Gobaine, Northboro, MA, makes NT 154 for high temperature applications.

[2] SN88 is a self-toughened grade of silicon nitride made by NGK Insulators, Nagoya, Japan for use at high temperatures.

[3] Certain commercial equipment, instruments or materials are identified in this paper in order to specify the experimental procedure adequately. Such identification is not intended to imply recommendation or endorsement by the National Institute of Standards and Technology, nor is it intended to imply that the materials or equipment identified are necessarily the best available for the purpose.

[4] Kyocera Corp., Kyoto, Japan, makes both SN 281 and SN 282.

Table 1
Summary of the creep tests performed on SN 281

Specimen	Temperature (°C)	Stress (MPa)	Creep rate (s^{-1})	Strain (%)	Lifetime (h)
77/24	1400	200	6.7×10^{-11}	0.5	>10200
77/19	400	280	4.1×10^{-10}	–	>4965
59/31	1450	200	1.4×10^{-9}	–	1380
59/32	1450	210	1.5×10^{-9}	–	643
59/36	450	230	2.5×10^{-9}	1.1	421
59/30	1450	255	6.1×10^{-9}	–	147
77/13	1500	184	2.6×10^{-9}	–	453
77/15	1550	184	7.4×10^{-9}	1.75	>546
77/14	1550	200	6.8×10^{-9}	2.5	>570
77/23	1550	220	1.9×10^{-8}	0.3	24.9

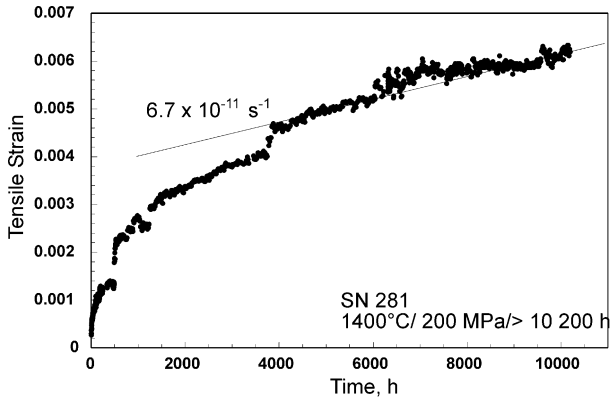

Fig. 1. Tensile creep curve obtained at 1400 °C under stress of 200 MPa in air indicate prolonged transient stage and the minimum rates below 1×10^{-10} s $^{-1}$.

which was determined as the difference between the densities of a sample from the gauge, ρ_{gauge} and a sample from the grip, ρ_{grip}:

$$f_v = (\rho_{grip} - \rho_{gauge})/\rho_{grip} \quad (1)$$

This procedure eliminates possible changes in the microstructure and density due to heat treatment in air. However, it cannot eliminate the effect of inhomogenieties in the as-received material. From error propagation theory and the repeatability of the density measurements (±0.00135 g/cm^2), the expected error in f_v is approximately ±0.000564.

2.4. Ultra-small-angle X-ray scattering

Four pairs of samples from the gauge and the corresponding grips, with dimensions of 2.5 mm×4 mm×0.15 mm, were cut from specimens deformed to strains of 0.5, 1.1, 1.75 and 2.50%. The grip-gauge pairs of specimens were compared to account for the initial porosity and possible changes in the microstructure induced by prolonged heat treatment. The cavity size distribution was determined from ultra-small-angle X-ray scattering (USAXS) data measured on beam line 33ID-D at the Advanced Photon Source at Argonne National Laboratory. Details of the USAXS instrument and evaluation of the anomalous USAXS data, which account for both the secondary phase and the porosity, are reported elsewhere.[25,26]

3. Results

3.1. Creep behavior

Nineteen specimens were tested in air at 1400, 1450, 1500 and 1550 °C at stresses ranging from 184 to 280 MPa, for periods of up to 10 200 h. Data from the creep experiments are summarized in Table 1. Two specimens broke during loading. Seven were interrupted prematurely due to failure in the gauge section, or breakage of the pins or tabs of the specimen. Therefore, of the 19 specimens tested, 10 gave data that were suitable for analysis.

Fig. 1 shows the tensile creep behavior of the material at 1400 °C under a stress of 200 MPa. The test was terminated prior to failure after 10 200 h. It was interrupted only once during this period due to a power outage. The total strain, ~0.5%, has an uncertainty of ~0.1% because of several interruptions in the data collection system. The transient stage exceeds 6000 h. The minimum strain rate in the last 6000 h of testing was estimated as 6.7×10^{-11} s^{-1}. Similar transient creep was observed at 1450 °C, whereas a more conventional behavior with the primary and secondary stages was observed at higher temperatures. To obtain an activation-energy, Q, and a stress exponent, n, from the creep data, a logarithmic form of the following equation was fitted to the data by the method of least squares:

$$\dot{\varepsilon} = \dot{\varepsilon}_o(\sigma/\sigma_o)^n \exp(-Q/RT) \quad (2)$$

where $\dot{\varepsilon}$ is the minimum creep rate, T is the temperature in K, R is the gas constant and σ is the applied stress. The constant, σ_o, is set equal to 1 MPa for dimensional purposes and the pre-exponential coefficient, $\dot{\varepsilon}_o$, is a constant of the fit having dimensions of s^{-1}. Values obtained for the present study were $\ln(\dot{\varepsilon}_o) = 3.6\pm9.5$, $n = 5.3\pm2.0$ and $Q = (757\pm117)$ kJ/mol. The standard deviation of the fit of $\ln(\dot{\varepsilon})$ upon σ and T is 0.694.

3.2. Material characterization

3.2.1. As-received material

The microstructure of the SN 281 (Fig. 2) consisted of Si_3N_4 matrix grains with a mean diameter of about 0.69 ± 0.10 μm. The grains appeared to be mainly equiaxed, however, a small number of the large grains

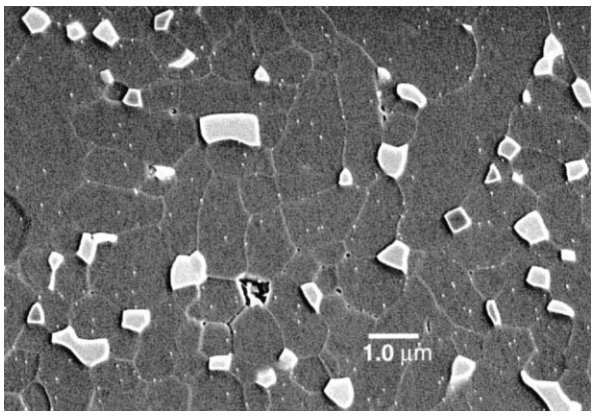

Fig. 2. This scanning electron micrograph was made by lightly plasma etching a polished section of SN281.

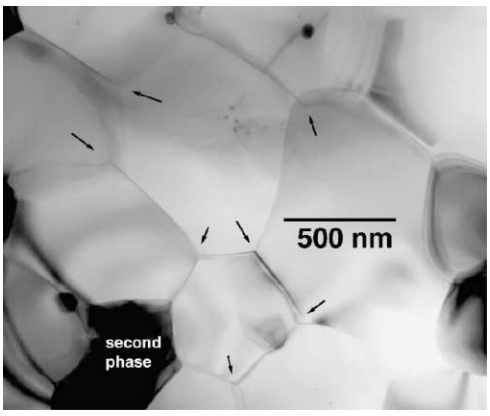

Fig. 4. Transmission electron micrograph shows that many of the triple junctions (arrows) within SN 281 contain no secondary phase.

of length up to 30 μm and diameters of 3–6 μm were dispersed throughout the microstructure. The secondary phases (7.3±2.5% by volume from the grips and 5.8±2.4% by volume from the gauges) were concentrated at the multigrain junctions (Fig. 2). Energy dispersive analysis (EDX) by transmission electron microscopy showed the presence of lutetium in the pockets originating from sintering additives (probably Lu_2O_3). Aside from Si, N, and O, no other elements were seen either in the pockets or at the grain boundaries. Subsequent X-ray diffraction analysis revealed the existence of monoclinic $Lu_2Si_2O_7$ (JCPDS cards No. 35–326, 34–509) and $Lu_4Si_2N_2O_7$ (JCPDS card No. 33–847) as the dominant crystalline secondary phases in the as-received material.[27] However, another modification of lutetium disilicate, triclinic B-$Lu_2Si_2O_7$ (JCPDS card No. 31–777), was found in some billets instead of monoclinic disilicate.

3.2.2. Microstructural changes after creep

Fig. 3 is a comparison of the X-ray diffraction patterns from the interior of the specimens after long-term creep at high temperatures. The same major secondary phases are present after 10 200 h exposure at 1400 °C and 520 h at 1550 °C as are found in the as-received material. This agrees with the absence of any visual changes due to oxidation. The oxidation layer on the specimen surface is approximately 10–20 μm thick even after the prolonged tests at 1550 °C.

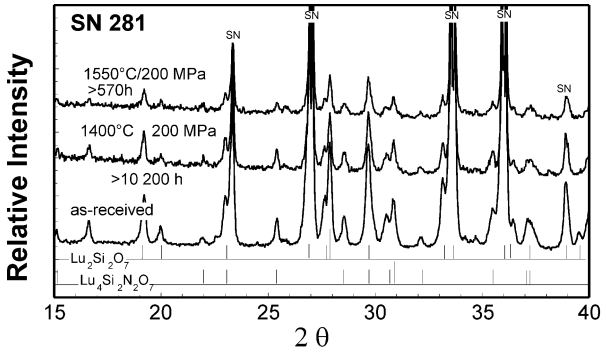

Fig. 3. X-ray diffraction study revealed $Lu_2Si_2O_7$ and $Lu_4Si_2N_2O_7$ as the crystalline secondary phases in the silicon nitride studied contains. Phase composition is stable even after 10 000 h at 1400 °C in air.

In agreement with our SEM observations, TEM observation of thin foils of the creep-tested specimens revealed that many of the triple junctions contained no secondary phase (Fig. 4). Multiple EDX analysis confirmed that Lu was the dominant constituent in the pockets. A very small Lu peak could be detected in the silicon nitride grains themselves, but at a much lower concentration than in the pockets or grain boundaries. This observation contrasts with other studies we made on Y or Yb containing silicon nitrides; we observed no lanthanides within the grains of these materials. A stronger peak of Lu appeared in the EDX spectra taken with the same spot size in the area including a boundary between two silicon nitride grains. Thus, a thin Lu-containing intergranular film or an adsorbed layer is present at the grain boundaries.

The grain boundaries were curved and twisted, making an analysis of the grain boundary thickness difficult. The boundaries that we could align parallel to the electron beam ranged in thickness from about 0.5 to 1 nm, which is typical of boundaries in crept materials (Fig. 5a). Such thickness variations in crept silicon nitride have been reported by others and related to the viscous flow of the amorphous phase during grain boundary sliding.[28] The boundary films between silicon nitride grains and secondary phase grains were up to 2 nm thick (Fig. 5b). The intergranular films were amorphous and continuous, and completely wetted all of the phases.

The crept SN 281 specimens had an unusually low volume fraction of cavities compared to other grades of silicon nitride. For example, fewer than 10 cavities were found in a thin foil prepared from the sample deformed to ~2.5%, whereas hundreds of cavities were typically observed in SN 88 silicon nitride at comparable strains.[11–13,15–17,29] Cavities that we did see varied in

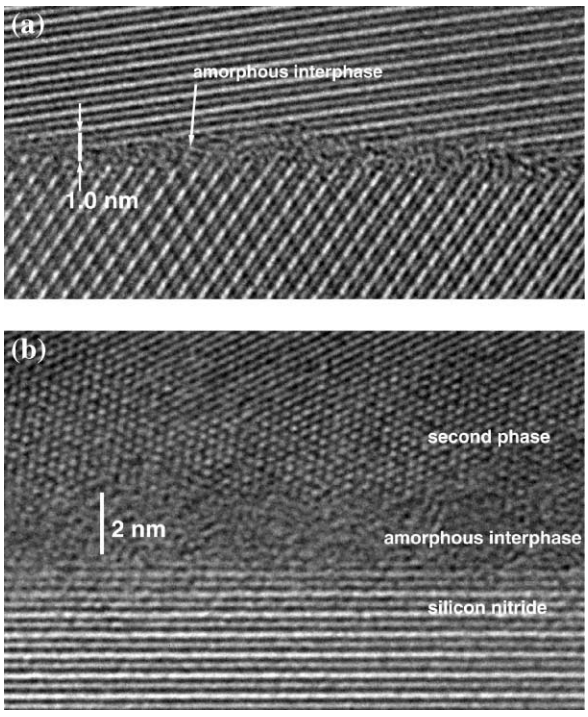

Fig. 5. High resolution electron microscopy micrographs of grain boundaries in SN 281: (a) an amorphous intergranular film between two silicon nitride grains with the thickness less than 1 nm after creep at 1550 °C up to 2.5%; (b) glassy film with the thickness of approximately 2 nm between silicon nitride and secondary phase grains.

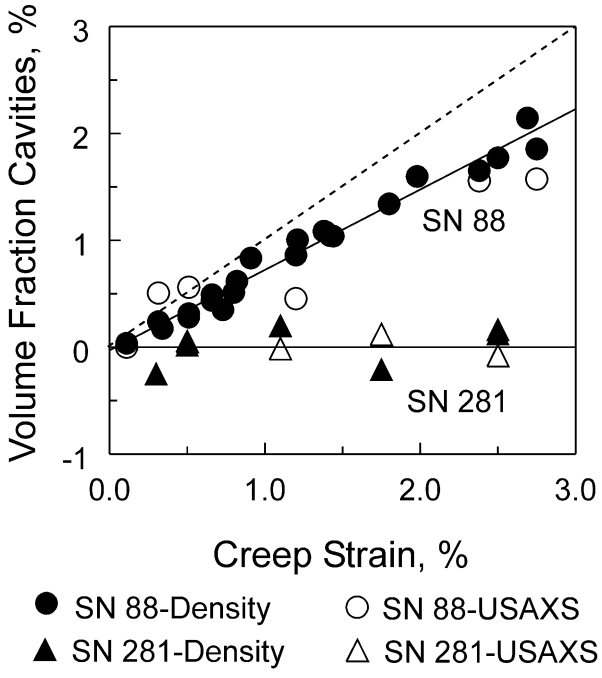

Fig. 6. A comparison of the dependencies between strain and volume fraction of cavities determined from USAXS and density change measurements in SN 281 and SN 88.[16,30] The contribution of cavities to tensile strain in SN 281 is close to zero while it is around 70% in SN 88.

size from 50 to 400 nm, which is the same range as the size of the secondary phase pockets.

By USAXS analysis, the SN 281 specimens displayed almost no porosity, in either the grip or the gauge. Fig. 6 is a summary of the USAXS results showing the dependence of the volume fraction of cavities on strain. The data indicate that the volume fraction of cavities is very low compared to the strain, which agrees with TEM observations. The occurrence of very small positive and negative values for f_v, consistent with $f_v = 0$, is an indication of the uncertainty in the results which is ± 0.002.

3.2.3. Direct density measurements

Fig. 6 also shows the dependence between the volume fraction of cavities and tensile strain in SN 281 measured by the sink–float technique. Two data points were obtained for the specimen strained to 2.5% to indicate the uncertainty in the density measurement. The data for the density change scatter about the strain axis indicating a negligible dependence on strain, in agreement with USAXS data and TEM observations. Data obtained on Yb/Y containing silicon nitride, SN 88[13,30] are also plotted in Fig. 6 as a comparison to the current set of data. The linear equations fitted to the SN 88 data give the line with a slope of 0.72 in the case of density measurement [13,30] and approximately the same value for USAXS measurement.[26]

4. Discussion

4.1. Comparison of creep resistance

The creep resistance of SN 281 at 150 MPa is much higher than that of other commercial grades of silicon nitride (Fig. 7). A maximum allowable strain of 1% in 10 000 h is considered to be a critical design limit for components designed for gas turbines.[17] If the strain exceeds this limit, rotating and moving parts stand in danger of rubbing or binding. Over a 10 000 h period, this strain corresponds to a strain rate of $\approx 3 \times 10^{-10}$ s^{-1}. Fig. 7 can be used to estimate the maximum temperature allowed at a stress of 150 MPa to achieve a strain of 1% in 10 000 h. For SN 281, this temperature is about 1470 °C. This temperature is about 230 °C higher than that for SN 88, 130 °C higher than that of NT154 and 100 °C higher than AS950EXP[5],[31] an experimental grade of material with nanoparticles of SiC at the grain boundaries. Only one successful tensile creep measurement has been carried out on silicon nitride sintered without additives.[32] This measurement can be used as a reference for the creep behavior of silicon nitride since it

[5] AS950EXP is a designation for an early version of AS950, Honeywell.

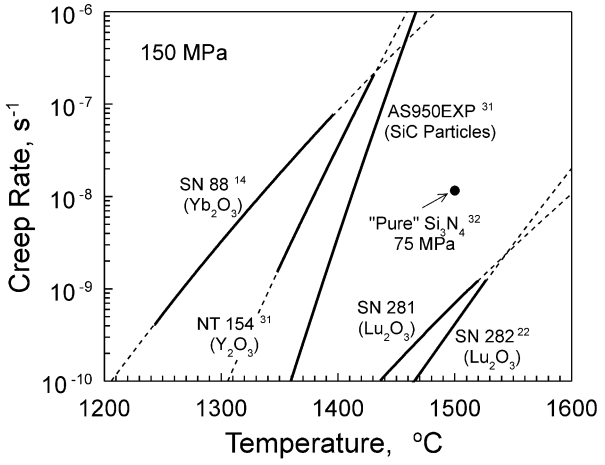

Fig. 7. A comparison of the temperature dependence of creep rates in SN 281 and SN 282[22] with earlier generations of silicon nitride with different rare-earth additives normalized to the stress of 150 MPa according to Eq. (2). The data point for the reference silicon nitride without sintering aids corresponds to 75 MPa.[32].

contains pure oxynitride glass at the grain boundaries.[33] At 1500 °C and 75 MPa, the minimum strain rate of the silicon nitride sintered without additives was 1.16×10^{-8} s^{-1}; the failure time was 203 h.[32] This strain rate is approximately 17 times greater than that for SN 281 at 150 MPa. If the creep rate of the SN 281 is extrapolated to 75 MPa, then the creep rate of the silicon nitride without additives at the same temperature and stress is approximately 63 times that of the SN 281.

Ohji studied the tensile creep behavior of a gas-pressure-sintered modification of SN281 designated SN 282.[22] These two grades of silicon nitride reportedly have the same chemical composition. A fit of Eq. (2) to Ohji's data yields the following values for the constants:[6] $\ln(\dot{\varepsilon}_o) = -6.44\pm6.01$; $n = 11.5\pm0.8$; $Q = (1074\pm74)$ kJ/mol. The stress exponent for SN 282 is higher than that for SN 281, 11.5 vs. 5.3, as was the activation energy, 1074 vs. 757 kJ mol^{-1}. Because the two sets of data had different stress dependencies, the SN 282 creeps slightly faster than SN 281 at higher stresses.

4.2. Cavitation vs. non-cavitation creep

SN 281 differs from other grades of silicon nitride because it deforms without cavitation. In the absence of cavitation, the deformation is non-dilatational, which implies that only non-dilatational mechanisms contribute to the creep. These include solution precipitation,[34–38] grain boundary sliding[39] and deformation by dislocation motion.[40] The latter is not a likely mechanism for the creep of silicon nitride, because the kinds of dislocations structures that are consistent with dislocation creep, pileups, etc., are not seen in silicon nitride deformed by creep.[41–48] Therefore, only two mechanisms can be active in SN 281, solution precipitation and grain boundary sliding. Since each of these mechanisms acting alone results in cavity formation, they must occur together to avoid cavitation.[40]

The absence of cavities suggests that diffusion can occur fast enough in SN281 to prevent the build-up of stresses that cause cavities to form in the silicate phase pockets. As creep occurs, the grains must be able to change their shape by grain boundary diffusion to maintain intergranular continuity. The slower of the two creep processes, sliding or diffusion, is the one that will be the rate-limiting step for creep. Regardless of which mechanism controls creep, n is expected to have a value of 1 or 2, provided both sliding and diffusion can be treated as linear processes with regard to the applied stress. The fact that the stress exponent for the creep rate is 5.3 suggests that a non-linear process is occurring in SN 281.

The higher stress exponent, n, observed for SN 281 can be justified by a mechanism suggested by Gasdaska,[39] whose model is based on viscous breakdown of the intergranular amorphous phase during deformation. Viscous breakdown of glass is a property in which the viscosity of the glass decreases as the shear rate increases. The phenomenon has been observed by several investigators and is predicted to occur at high rates of shear.[49] Gasdaska assumed sliding along grain boundaries controlled the creep of silicon nitride. As the creep rate increased, the viscosity of the amorphous phase decreased, yielding the kind of behavior observed experimentally.[50]

Luecke and Wiederhorn[13] raised a serious objection to this theory based on the behavior of silica glass, one of the most viscous glasses at high temperature. Using the same assumptions as were used by Gasdaska, they modeled the creep behavior of silicon nitride and calculated the strain rate of the intergranular amorphous phase. The calculation showed that the strain rate was only one-thousandth that required for viscous breakdown in bulk silica glass. Consequently, the glass at the grain boundaries should still have been in the Newtonian range of behavior. The glass found at grain boundaries in silicon nitride will not be pure silica or a nitrogen-silica glass, but will contain sintering aids that significantly lower the glass viscosity. Hence, an even higher creep rate will be needed for non-Newtonian behavior.

4.3. Lu_2O_3 in glass

Understanding the role of Lu_2O_3 in the amorphous phase is also problematic. If the effect of Lu was primarily its effect on the viscosity of the amorphous phase

[6] Differences between the SN 281 and SN 282 in Fig. 6 and a similar Figure in Ref. 21 are due to the use of Eq. (2) instead of the formula for cavitation creep developed by Luecke and Wiederhorn.[13]

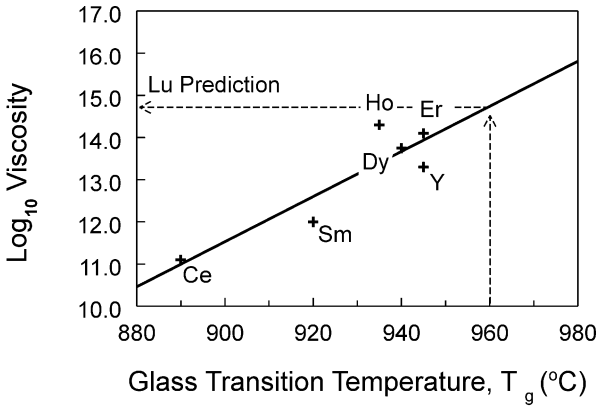

Fig. 8. Prediction of viscosity from the glass transition temperature. The data is taken from Ramesch et al.[52] The glass transition temperatures, T_g, and viscosities at 900 °C for these glasses were obtained from Ref. 52.

at the grain boundaries, then the higher resistance to creep might be explained by a change in composition of the grain boundaries. The effect of rare-earth oxides on glass transition temperature, T_g, or on viscosity has been studied on oxynitride glasses by a number of authors[51–53]

Ramesh et al.[52] measured a variety of physical properties (including the glass transition temperature, T_g, and the viscosity) of glasses containing 17% equivalent fraction nitrogen and Y, Ce, Nd, Sm, Eu, Dy, Ho and Er as additives. With the exception of Eu,[7] the properties of the glasses varied linearly with cationic field strength of the rare-earth oxide. All glasses contained 16% equivalent fraction Al in the structure. Direct measurements demonstrated a three order of magnitude change in viscosity with the change in rare earth oxide at 900 °C (Fig. 8). For the same series, T_g increased by 55 °C from about 890 °C to 945 °C. Neither Yb nor Lu were used in the study. This study demonstrates a large change of viscosity over the range of variation of rare-earth oxide. It also demonstrates a strong correlation between T_g and viscosity at a given temperature.

Becher et al.[53] carried out a study using rare-earth oxides that only exhibited a valence of +3. Their study included Lu, but not Yb (which can have a +2 charge). Four glass types were studied; two were free of nitrogen. The other glasses had a concentration of either 20 or 30% equivalent fraction nitrogen. In general, their measurements of T_g were in agreement with those made in earlier studies.[51,52] For the nitrogen containing glasses, the T_g increased by approximately 50 °C from La to Lu, which was about one-half the rate observed by Ramesh et al.[52]

The increase in viscosity when Lu is substituted for Y, can be estimated from the data of Ramesh et al.[52] A plot of T_g as a function of cationic field strength (from their paper, but not shown here) is extrapolated to estimate a T_g of about 960 °C for Lu.[8] Viscosities at 900 °C, from the paper by Ramesh et al., are then plotted as a function of T_g, and the value of T_g for Lu is used to determine a value of the viscosity for a Lu containing glass (Fig. 8). The estimated increase in viscosity of 1.5 orders of magnitude is less than the approximately 3 orders of magnitude needed at 1400 °C to explain the differences in creep behavior shown in Fig. 7. Nevertheless, this substantial change in viscosity offers promise that under the right conditions, exchanging Lu for Y could increase viscosity enough to account for the observed creep behavior. The applicability of the glass data to the SN 281 may, however, be questioned because of the absence of Al in the sintering aid for this material.

Other features of the composition or microstructure of SN 281 may also affect its creep behavior. The viscosity of glass, for example, is strongly affected by the concentration of nitrogen ions in the glass,[53–57] a network former that strongly cross-links the glass network and increases its viscosity. The transition temperature in Y–Si–Al–O–N glass is increased by 70 °C and its viscosity by two orders of magnitude when the nitrogen content is increased from zero to 1.5% atom fraction.[55–57] Therefore, a small change in nitrogen concentration will have a large effect on viscosity. While these observations are intriguing, determination of the exact mechanism that results in the superior creep behavior of this material will have to await future investigation.

5. Conclusions

The creep resistance of silicon nitride containing Lu-doped additives is 3–5 orders of magnitude greater than those of the earlier grades containing Y- and/or Yb-additives. This material has a potential for prolonged operation at temperatures up to 1470 °C. The stress exponent, n, and the activation energy, Q, for creep are, 5.3 ± 2.0 and 757 ± 117 kJ mol^{-1}, respectively. Precise density and USAXS measurements revealed that, in contrast to other grades of silicon nitride, cavitation does not occur in SN 281. Redistribution of the secondary phases via solution precipitation accompanying grain boundary sliding was discussed as possible creep mechanism in SN 281. Replacement of Y by Lu and an associated increase in viscosity of the amorphous grain boundary phase may explain the changes in creep behavior.

[7] Eu does not fit the series and is believed to have a charge of +2 rather than +3.

[8] An Eu containing glass was included in the figure but was not used in the extrapolation

Acknowledgements

The UNICAT facility at the Advanced Photon Source, Argon National Laboratory is supported by the University of Illinois at Urbana/Champaign, Oak-Ridge National Laboratory (ORNL) and the National Institute of Standards and Technology (NIST). The U.S. Department of Energy, Basic Energy Sciences, supports the use of the Advanced Photon Source under contract No. W-31–109-ENG-38. F. Lofaj was supported by the Fulbright Commission and by NIST. L. Browder and J. Andreason were supported by the Illinois EXITE program. Discussions with W.E. Luecke (NIST) and P.F. Becher (ORNL), and creep data provided by T. Ohji (National Industrial Research Institute of Nagoya) are highly appreciated.

References

1. Broomfield, R. W., Ford, D. A., Bougher, J. K., Thomas, M. C., Frasier, D. J., Burkholder, P. S., Harris, K., Ericksson, G. L. and Wahl, J. D., Development and turbine engine performance of three advanced rhenium containing superalloys for single crystal and directionally solidified blades and vanes. *J. Eng. Gas Turbines Power, Trans. ASME*, 1998, **120**, 595–608.
2. Amagasa, S., Shimomura, K., Kadowaki, M., Takeishi, K., Kawai, H., Aoki, S. and Aoyama, K., Study on the turbine vane and blade for a 1500 °C class industrial gas turbine. *J. Eng. Gas Turbines Power, Trans. ASME*, 1994, **116**, 597–603.
3. Kizuka, N., Sagae, K., Anzai, S., Marushima, S., Ikeguchi, T. and Kawaike, K., Conceptual design of the cooling system for 1700 °C-class hydrogen fueled combustion gas turbines. *J. Eng. Gas Turbines Power, Trans. ASME*, 1999, **121**, 108–115.
4. Takehara, I., Tatsumi, T. and Ichikawa, Y., Development summary of CGT 302 ceramic gas turbine. In *Proc. of Int. Gas Turbine Congress 1999* Kobe, Gas Turbine Soc. Japan, Tokyo, Japan, 1999, pp. 57–64.
5. Yoshida, M., Tanaka, K., Tsuruzono, S. and Tatsumi, T., Development of silicon nitride components for ceramic gas turbine engine (CGT 302). *Ind. Ceramics*, 1999, **19**, 188–192.
6. Parthasarathy, V. M., van Roode, M., Price, J. R., Gates, S., Waslo, S. and Hoffman, P., Review of solar's ceramic stationery gas turbine development program. In *Proc. 6th Int. Symp. Ceramic Materials and Components for Engines*, ed. K. Niihara, S. Hirano, S. Kanzaki, K. Komeya and K. Morinaga. Technoplaza Co, Tokyo, Japan, 1997, pp. 259–264.
7. van Roode, M., Price, J. R., Jimenez, O., Miriyala, N. and Gates Jr., S., Design and testing of ceramic components for industrial gas turbines. In *Proc. 7th Int. Symp. Ceramic Materials and Components for Engines*, ed. J. G. Heinrich and F. Aldinger. Willey-VCH, Weinheim, Germany, 2001, pp. 261–266.
8. Mennon, M. N., Fang, H. T., Wu, D. C., Jenkins, M. G., Ferber, M. K., Moore, K. L., Hubbard, C. R. and Nolan, T. A., Creep and stress rupture behavior of an advanced silicon nitride: Part I, experimental observation. *J. Am. Ceram. Soc.*, 1994, **77**(5), 1217–1227.
9. Ferber, M. K., Jenkins, M. G., Nolan, T. A. and Yeckley, R. L., Comparison of the creep and creep rupture performance of two hiped silicon nitride ceramics. *J. Am. Ceram. Soc.*, 1994, **77**(3), 657–665.
10. Luecke, W. E., Wiederhorn, S. M., Hockey, B. J., Krause, R. E. Jr. and Long, G. G., Cavitation contributes substantially to tensile creep in silicon nitride. *J. Am. Ceram. Soc.*, 1995, **78**(8), 2085–2096.
11. Wiederhorn, S. M., High temperature deformation of silicon nitride. *Z. Metallkd.*, 1999, **9**(12), 1053–1058.
12. Lofaj, F., Cao, J.-W., Okada, A. and Kawamoto, H., Comparison of creep behavior and creep damage mechanisms in the high performance silicon nitrides. In *Proc. 6th Int. Symp. Ceramic Materials and Components for Engines*, ed. K. Niihara, S. Hirano, S. Kanzaki, K. Komeya and K. Morinaga. Technoplaza Co., Inc, Tokyo, Japan, 1997, pp. 713–718.
13. Luecke, W. E. and Wiederhorn, S. M., A new model for tensile creep of silicon nitride. *J. Am. Ceram. Soc.*, 1999, **82**(10), 2769–2778.
14. Krause, R. F. Jr., Luecke, W. E., French, J. D., Hockey, B. J. and Wiederhorn, S. M., Tensile creep and rupture of silicon nitride. *J. Am. Ceram. Soc.*, 1999, **82**(5), 1233–1241.
15. Lofaj, F., Tensile creep behavior in an advanced silicon nitride. *Mater. Sci. Eng. A*, 2000, **279**(1–2), 61–72.
16. Yoon, K. J., Wiederhorn, S. M. and Luecke, W. E., A comparison of tensile and compressive creep behavior in silicon nitride. *J. Am. Ceram. Soc.*, 2000, **83**(8), 2017–2022.
17. Wiederhorn, S. M., Lifetime prediction for silicon nitride. In *Proc. 7th Int. Symp. Ceramic Materials and Components for Engines*, ed. J. G. Heinrich and F. Aldinger. Willey-VCH, Weinheim, Germany, 2001, pp. 109–114.
18. Kaji, M., Ono, T., Higashi, M. and Kokaji, A., Stress rupture behavior of silicon nitride under combustion gas environment. In *Proc. of 1995 Yokohama Int. Gas Turbine Congress*, Nissei Ebro, Inc., Tokyo, Japan, 1995, pp. III-21–III-28.
19. Lofaj, F., Wiederhorn, S. M., Long, G. G., Jemian, P. R. and Ferber, M. K., Cavitation creep in the next generation silicon nitride. In *Proc. 7th Int. Symp. Ceramic Materials and Components for Engines*, ed. J. G. Heinrich and F. Aldinger. Willey-VCH, Weinheim, Germany, 2001, pp. 487–493.
20. Lofaj, F., Wiederhorn, S. M., Long, G. G. and Jemian, P. R., Tensile creep in the next generation silicon nitride. *Ceram. Eng. and Sci. Proc.*, 2001, **22**, 167–174.
21. Lofaj, F., Okada, A., Ikeda, Y. and Kawamoto, H., Creep processes in the advanced silicon nitride ceramics. *Key Eng. Materials*, 2000, **171–174**, 747–754.
22. Ohji, T., Long-term tensile creep behavior of highly creep resistant silicon nitride for ceramic gas turbines. In *Ceramic Processing Science*, ed. S. H. Hirano, G. L. Messing and N. E. Claussen. Ceram. Trans, 2000.
23. French, J. D. and Wiederhorn, S. M., Tensile specimens from ceramic components. *J. Am. Ceram. Soc.*, 1996, **79**(2), 550–552.
24. DeHoff, R. T. and Rhines, F. N., *Quantitative Microscopy*. McGraw-Hill, New York, 1968.
25. Long, G. G., Allen, A. J., Ilavsky, J., Jemian, P. R. and Zschack, P., The Ultra-Small-Angle X-ray Scattering Instrument on UNICAT at the APS. In *CP 521, Synchrotron Radiation Instrumentation: 11th US National Conf.*, ed. P. Pianetta, J. Arthur and S. Brennan. American Institute of Physics, USA, 2000, pp. 183–187.
26. Jemian, P. R., Long, G. G., Lofaj, F. and Wiederhorn, S. M., Anomalous ultra-small-angle X-ray scattering from evolving microstructures during creep. In *MRS Symp. 590, Applications of Synchrotron Radiation Techniques to Materials Scien*ce V, ed. S. R. Stock, S. M. Mini and D. L. Perry. MRS, 2000, pp. 131–136.
27. *Powder Diffraction File*, International Centre for Diffraction Data, 1601 Park Lane, Swarthmore, PA 19081–2389.
28. Jin, Q., Wilkinson, D. S. and Weatherly, G. C., High-resolution electron microscopy investigation of viscous flow creep in a high purity silicon nitride. *J. Am. Ceram. Soc.*, 1999, **82**(6), 1492–1496.
29. Lofaj, F., Usami, H., Okada, A. and Kawamoto, H., Creep damage in an advanced self-reinforced silicon nitride: Part I, cavitation in the amorphous phase. *J. Am. Ceram. Soc.*, 1999, **82**(4), 1009–1019.

30. Lofaj, F., Blessing, G. V. and Wiederhorn, S. M., Ultrasound velocity technique for non-destructive quantification of elastic moduli degradation during creep in silicon nitride. *J. Am. Ceram. Soc.*, in press.
31. Krause, R. F. Jr., Wiederhorn, S. M. and Li, C.-W., Tensile creep behavior of a gas-pressure sintered silicon nitride. *J. Am. Ceram. Soc.*, 2001, **84**(10), 2394–2400.
32. Luecke, W.E., personal communication, 2000.
33. Tanaka, I., Pezzotti, G., Okamoto, T. and Miyamoto, Y., Hot isostatic pressing of silicon nitride without additives. *J. Am. Ceram. Soc.*, 1989, **72**(9), 1656–1660.
34. Pharr, G. M. and Ashby, M. F., On creep enhanced by a liquid phase. *Acta Metall.*, 1983, **31**, 129–138.
35. Tsai, R. L. and Raj, R., Creep fracture in ceramics containing small amounts of a liquid phase. *Acta Metall.*, 1982, **30**, 1043–1058.
36. Raj, R. and Chyung, C. K., Solution-precipitation creep in glass ceramics. *Acta Metall.*, 1981, **29**, 159–186.
37. Wang, J. G. and Raj, R., Mechanism of superplastic flow in a fine-grained ceramic containing some liquid phase. *J. Am. Ceram. Soc.*, 1984, **67**, 399.
38. Wakai, F., Step model of solution-precipitation creep. *Acta Metall. Mater.*, 1994, **42**(4), 1163–1172.
39. Gasdaska, C. J., Tensile creep in an *in situ* reinforced silicon nitride. *J. Am. Ceram. Soc.*, 1994, **77**(9), 2408–2418.
40. Poirier, J.-P., *Creep of Crystals*. Cambridge University Press, Cambridge, England, 1995.
41. Luecke, W. E., Wiederhorn, S. M., Hockey, B. J., Krause Jr., R. and Long, G. G., Cavitation contributes substantially to tensile creep in silicon nitride. *J. Am. Ceram. Soc.*, 1995, **78**(8), 2085–2096.
42. Kossowsky, R., Miller, D. G. and Diaz, E. S., Tensile and creep strengths of hot pressed Si_3N_4. *J. Mater. Sci.*, 1975, **10**, 983–997.
43. Lange, F. F., Davis, B. I. and Clarke, D. R., Compressive creep of Si_3N_4/MgO alloys, Part 1, effect of composition. *J. Mater. Sci.*, 1980, **15**, 601–610.
44. Crampon, J., Duclos, R. and Rakotoharisoa, N., Compression creep of $Si_3N_4/MgAl_2O_4$ alloys. *J. Mater. Sci.*, 1990, **25**, 1203–1208.
45. Crampon, J., Duclos, R. and Rakotoharisoa, N., Creep behavior of $Si_3N_4/Y_2O_3/Al_2O_3$/AlN alloys. *J. Mater. Sci.*, 1993, **28**, 909–916.
46. Bernard-Granger, G., Crampon, J., Duclos, R. and Cales, B., High temperature creep behaviour of β'-Si_3N_4/α-YSiAlON ceramics. *J. Eur. Ceram. Soc.*, 1997, **17**, 1647–1654.
47. Birch, J. M. and Wilshire, B., The compression creep behaviour of silicon nitride ceramics. *J. Mater. Sci.*, 1978, **13**, 2627–2636.
48. Koester, D. A., More, K. L. and Davis, R. F., Deformation and microstructural changes in SiC-whisker-reinforced Si_3N_4 composites. *J. Mater. Res.*, 1991, **6**, 2735–2746.
49. Eyring, H., Viscosity, plasticity, and diffusion as examples of absolute reaction rates. *J. Chem. Phys.*, 1936, **4**, 286–291.
50. Li, J. H. and Uhlmann, D. R., The flow of glass at high stress levels, I non-newtonian behavior of homogeneous 0.08 Rb_2O-0.92 SiO_2 glasses. *J. Non-Crystalline Solids*, 1970, **3**, 127–147.
51. Ohashi, M., Nakamura, K., Hirao, K., Kanzaki, S., Hampshire, S. and Formation, properties of Ln-Si-O-N glasses (Ln = Lanthanides or Y), *J. Am. Ceram. Soc.*, 1995, **78**(1), 71–76.
52. Ramesh, R., Nestor, E., Pomeroy, M. J. and Hampshire, S., Formation of Ln-Si-Al-O-N glasses and their properties. *J. Eur. Ceram. Soc.*, 1997, **17**, 1933–1939.
53. Becher, P. F., Walters, S. B., Westermoreland, C. G. and Riester, L., Compostional effects on the properties of Si-Al-RE bases oxynitride glasses (RE = La, Nd, Gd, Y, or Lu). *J. Am. Ceram. Soc.*, 2002, **85**, 897–902.
54. Doremus, R. H., *Glass Science*. John Wiley and Sons, Inc, New York, 1973.
55. Loehman, R. E., Oxynitride glasses. In *Treatise on Materials Science and Technology, Glass IV*, ed. M. Tomozawa and R. H. Doremus. Academic Press, Orlando, USA, 1985, pp. 119–149.
56. Rouxel, T., Huger, M. and Besson, J. L., Rheological properties of Y-Si-Al-O-N glasses—elastic moduli, viscosity and creep. *J. Mater. Sci.*, 1992, **27**, 279–284.
57. Lemercier, H., Rouxel, T., Fargeot, D., Besson, J. L. and Piriou, B., Yttrium SIAlON glasses: structure and mechanical properties—elasticity and viscosity. *J. Non-Cryst. Solids*, 1996, **201**, 128–145.